



*Supplement of*

## **Topographic disequilibrium, landscape dynamics and active tectonics: an example from the Bhutan Himalaya**

**Martine Simoes et al.**

*Correspondence to:* Martine Simoes (simoes@ipgp.fr)

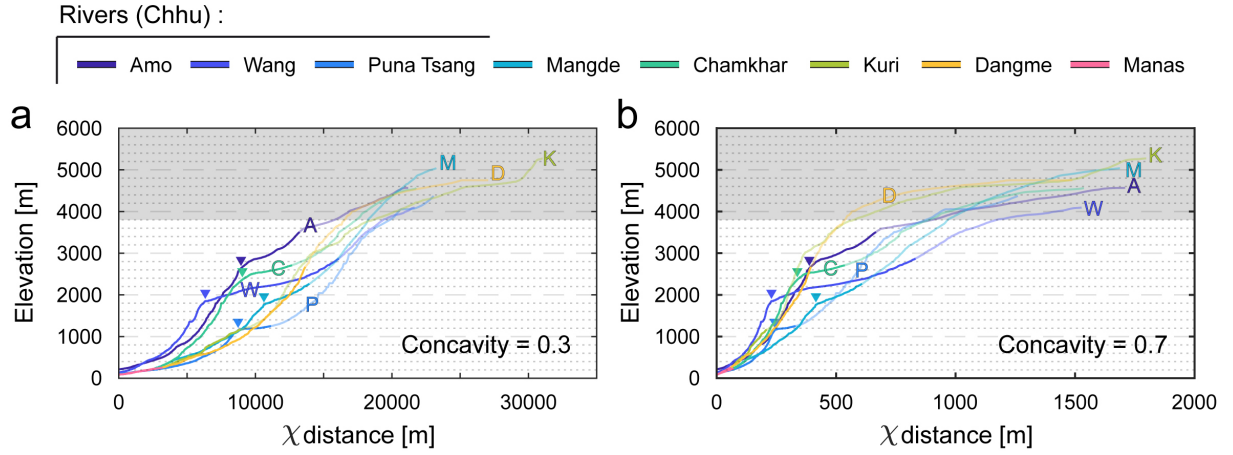
The copyright of individual parts of the supplement might differ from the article licence.

This supplementary material provides figures complementary to those presented in the main manuscript.

More specifically, Figures S3 and S6 compare  $\chi$  metrics with other Gilbert metrics within and around the Bumthang and Phobjika regions, as a complement to Figures 7 and 9 of main text. Similarly, Figures S4 and S7 present the same metrics within and around the Wang and Yarab low-relief regions (location of these regions on Figure 1 in main text). Similarly, Figure S8 presents longitudinal and transformed profiles of rivers draining or surrounding the Yarab low-relief region, following the approach of Yang et al. (2015), as also done for rivers within and round the Phobjika area in Figure 8.

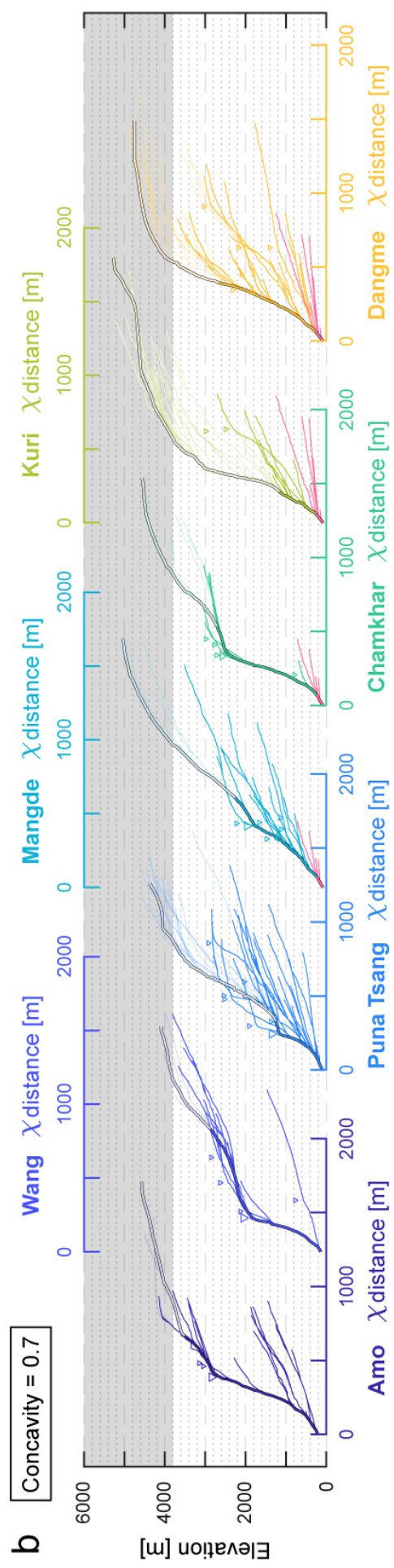
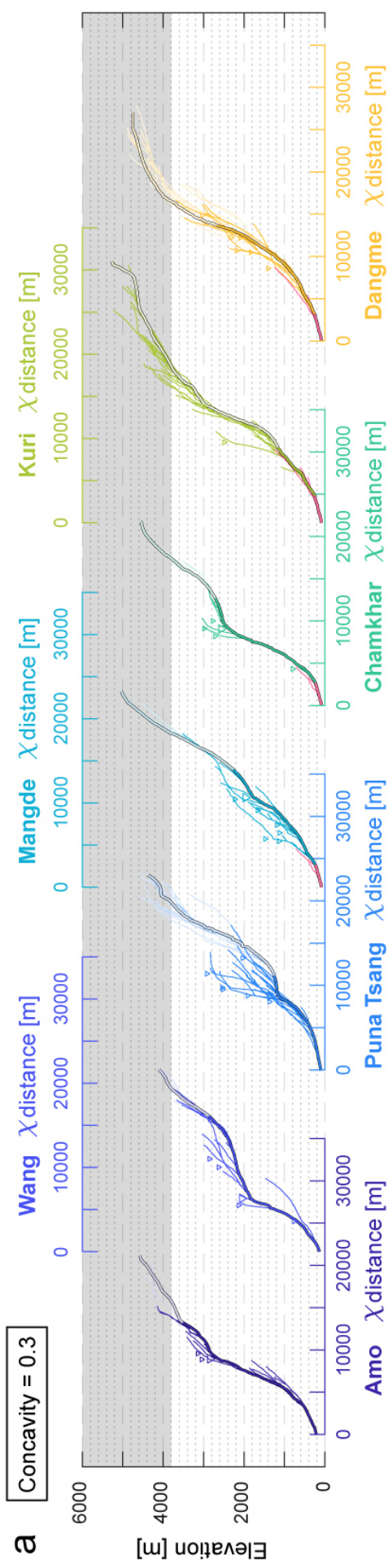
Additionally, supplementary figures are presented to illustrate transformed river profiles for concavities others than the value of 0.5 chosen for figures in the main text. As such, Figures S1, S2, S5 and S9 test the effects of concavity values of 0.3 and 0.7 on transformed river profiles, and should be compared to Figures 5, 6, 8 in the main text, and Figure S8 in supplementary material.

Finally, Figure S10 confirms the absence of a simple correlation between upstream knickpoint position (relative to base level), knickpoint altitude and drainage area in the case of major and large rivers.



**Figure S1: Transformed river profiles of majors and large rivers in Bhutan**, following the formalism of Perron and Royden (2013). Rivers are located on the maps of Figure 1 (Main text), and are color-coded and labeled. Major knickpoints are also pointed by triangles. Regions with altitudes above 3800 m (grey area) are not to be compared directly to the downstream sections as these may have a glacial imprint. Portions of the rivers north of physiographic transition T3 are reported by transparent segments. The Gangetic Plain is used as the base level for all these rivers.  $\chi$  transformed profiles are established here with a concavity of 0.3 (a - left panel) and 0.7 (b - right panel), as a complement to the profiles of Figure 5b where a concavity of 0.5 is considered. As noted on Figure 5b, river profiles are discordant. A: Amo Chhu; W: Wang Chhu; P: Puna Tsang Chhu; M: Mangde Chhu; C: Chamkhar Chhu; K: Kuri Chhu; D: Dangme Chhu.

**Figure S2 (next page): Transformed river profiles of major rivers in Bhutan and of their tributaries** (with drainage area  $> 50 \text{ km}^2$ ) (Location in Figure 1). Major drainage basins (and the corresponding horizontal axes of their profiles) are color-coded as in Figure 1. Trunk streams are reported in bold lines, and tributaries in thinner lines. Lighter colors are used along river profiles for the river portions north of physiographic transition T3. Major knickpoints are pointed out by triangles. Altitudes above 3800 m are considered aside (grey band) as rivers may preserve a glacial imprint in these regions.  $\chi$  transformed profiles are established with a concavity of 0.3 (a - top) and 0.7 (b - bottom), as a complement to the transformed profiles shown in Figure 6b where a concavity of 0.5 is considered. In the case of a concavity of 0.7, there exist tributaries that plot below the transformed profile of their trunk stream, even though these tributaries are those gaining drainage area by divide migration around high-altitude low-relief regions.



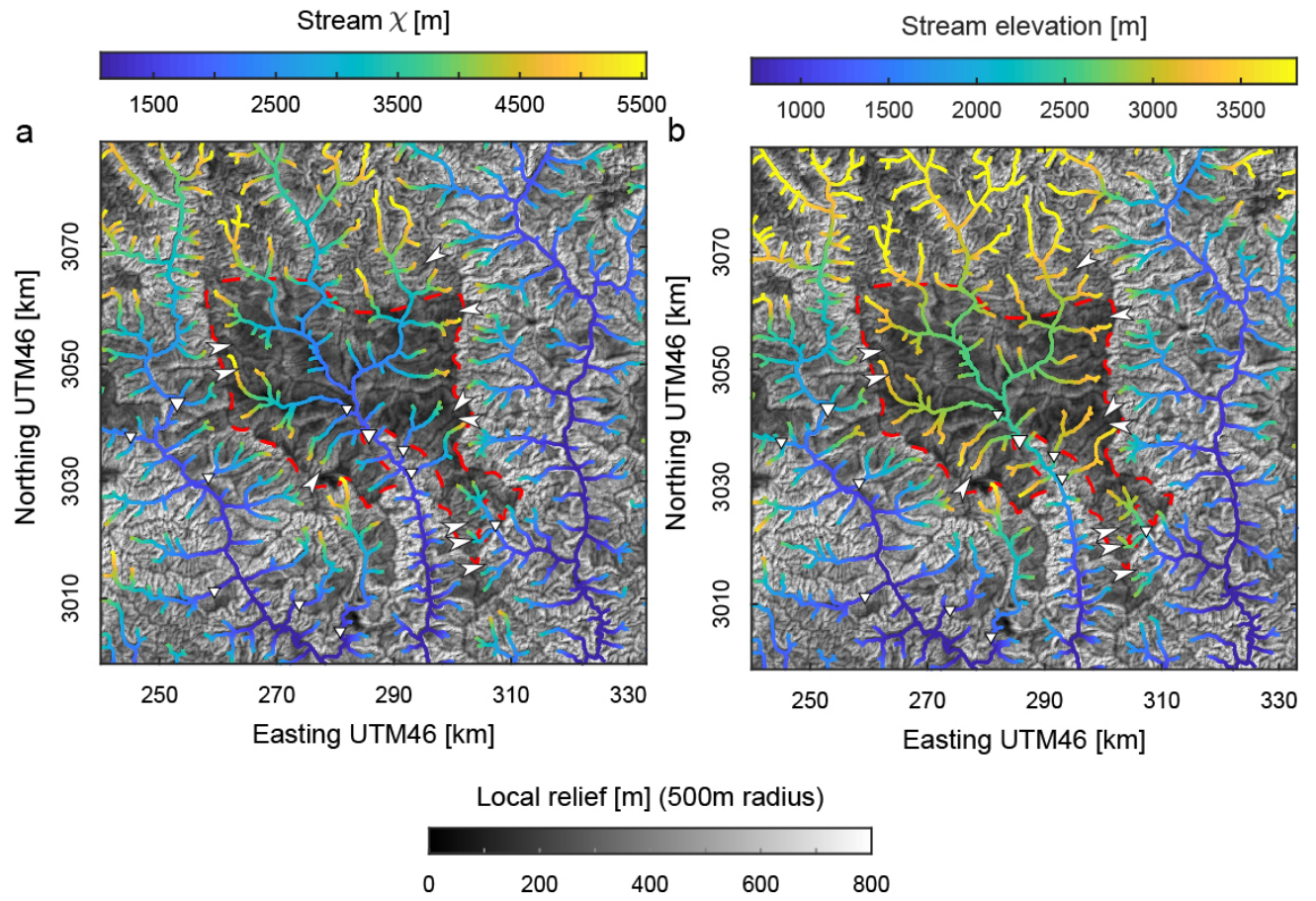


**Figure S3: Assessing divide mobility around the high-altitude low-relief Bumthang region crossed by the Chamkhar Chhu** (see Figure 1c for location), as in theoretical Figure 4d. Map represents local relief, with a moving window of 500 m. The red dashed line gives the limit of the identified low-relief region. Major knickpoints are reported with inversed triangles and arrows locate the existence of morphological observations of regressive erosion (wind gaps), together with the direction of the associated divide migration. Similar observations are reported for the Wang surface (Figure S4).

a)  $\chi$  along the river network as a criterium to assess divide mobility (following (Willett et al., 2014)). The values of  $\chi$  are determined for a concavity of 0.5. Same as map in Figure 7 (main text).

b) Stream elevation as a criterium to assess divide mobility (following (Forte and Whipple, 2018; Whipple et al., 2017b)).



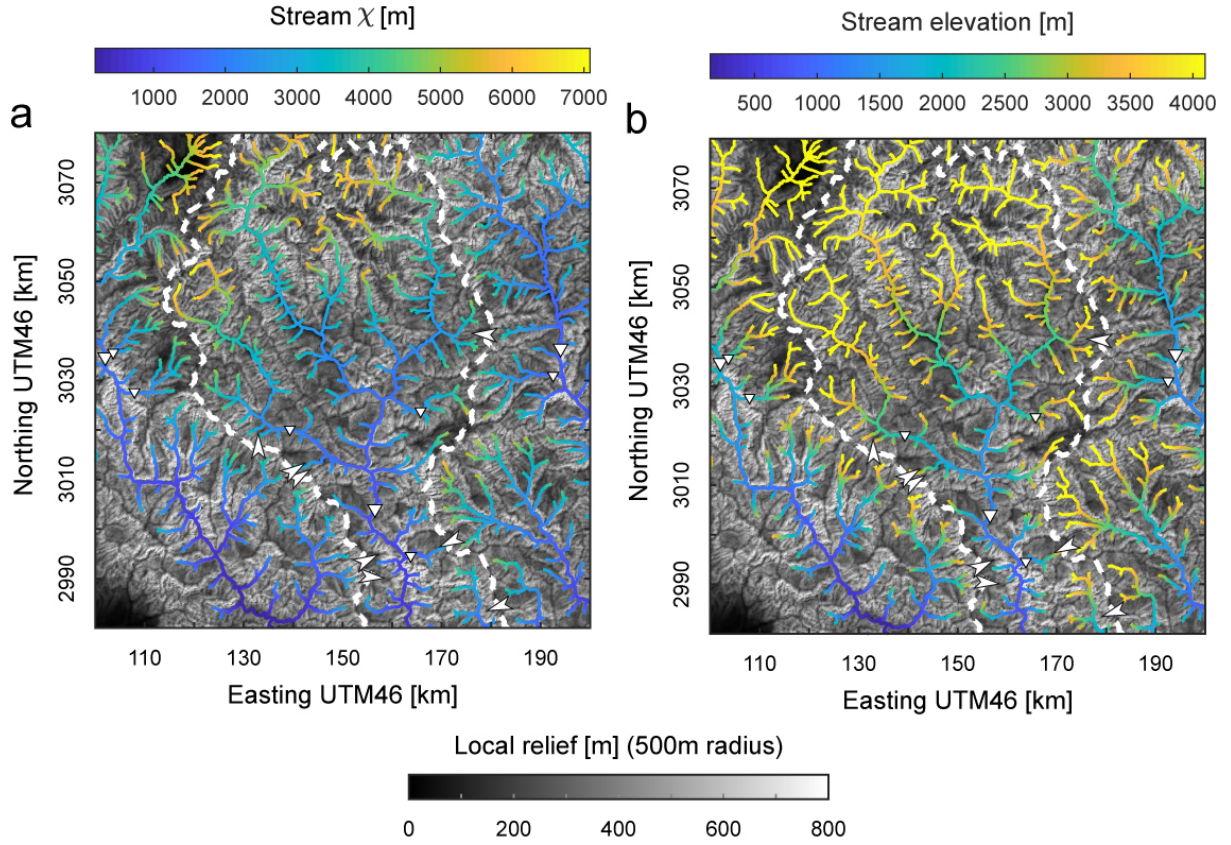


**Figure S4: Assessing divide mobility around the high-altitude low-relief region around the Wang Chhu** (see Figure 1c for location), to be compared with Figure S3 where the same approach is followed for the Bumthang surface. Map represents local relief, with a moving window of 500 m. The white dashed line delineates the drainage basin of the Wang Chhu. Major knickpoints are reported with inversed triangles and arrows locate the existence of morphological observations of regressive erosion (wind gaps), together with the direction of the divide migration deduced from them.

a)  $\chi$  along the river network as a criterium to assess divide mobility (following Willett et al. (2014)). The values of  $\chi$  are determined for a concavity of 0.5.

b) Stream elevation as a criterium to assess divide mobility (following Forte and Whipple (2018), and Whipple et al. (2017)).

The case of the Wang surface is more complex than that of the Bumthang surface. Indeed, this low-relief region is not as clearly delimited as the other ones (Figure 1c). Gilbert metrics favor an inward migration of the eastern divide of the Wang Chhu (shared with the Puna Tsang Chhu) upstream of its major knickpoint, and an outward migration of this same divide downstream of the knickpoint. This latter deduction from Gilbert metrics is contrary to that from satellite observations from wind gaps south of the knickpoint. Such contradictory observations are also found along the western divide of the basin (shared with the Amo Chhu). We suggest that these conflicting deductions may reveal an unstability of the river network more extreme than further east, also deductible from several isolated patches with relatively lower-relief in this southwestern part of Bhutan (Figure 1c).

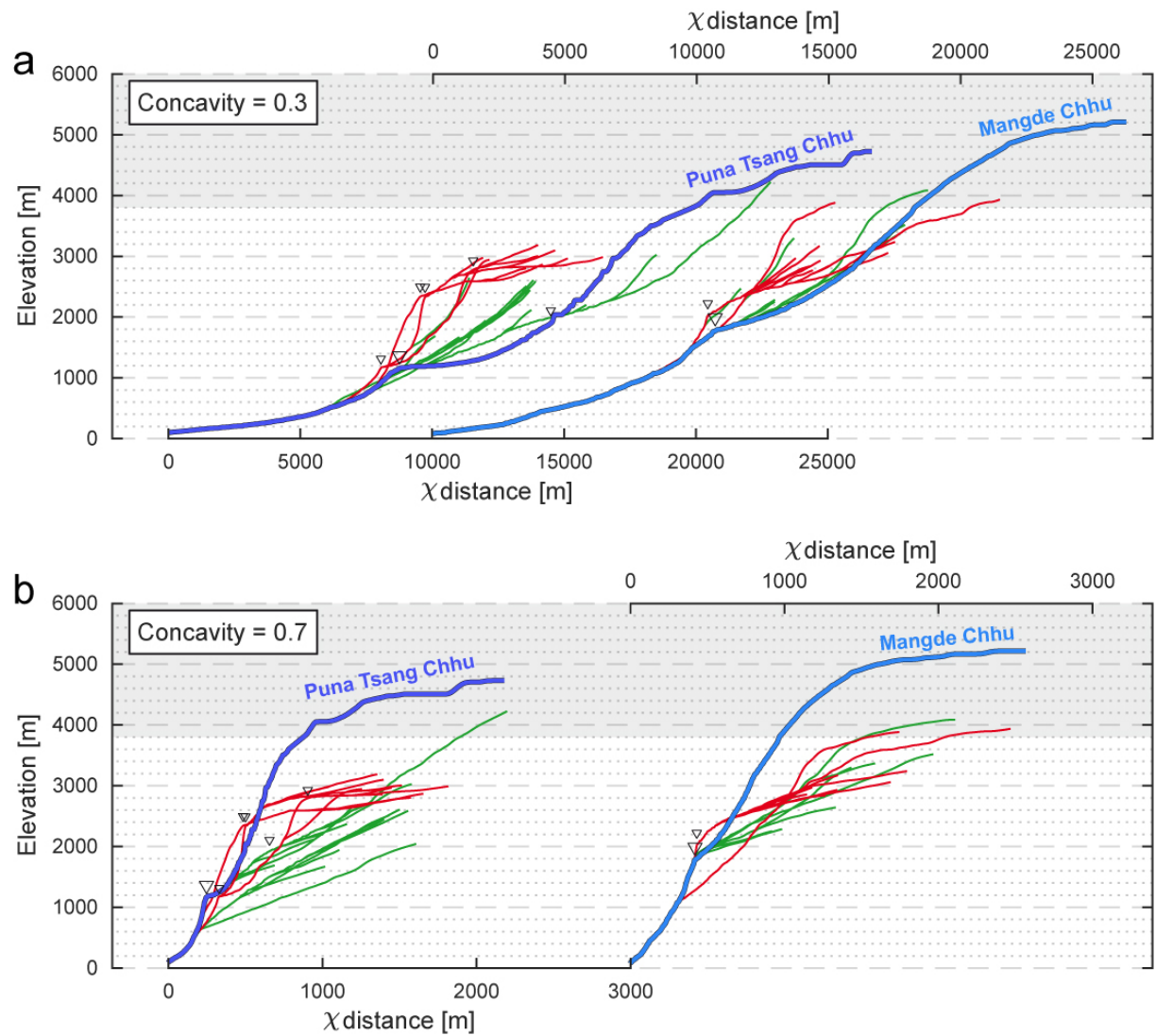


**Figure S5: Transformed river profiles around and within the Phobjika high-altitude low-relief surface,** following the approach of Yang et al. (2015) (see map of Figure 8 in main text). Concavity values of 0.3 (a- top) and 0.7 (b- bottom) are tested, complementing the transformed profiles of Figure 8c (main text) with a concavity of 0.5. Tributaries draining the low-relief region are represented in red. Tributaries external to the low-relief region are plotted in green. Main trunk streams of the Puna Tsang and Mangde Chhu are in blue. None of the profiles of the rivers draining the low-relief region (in red) are concordant.

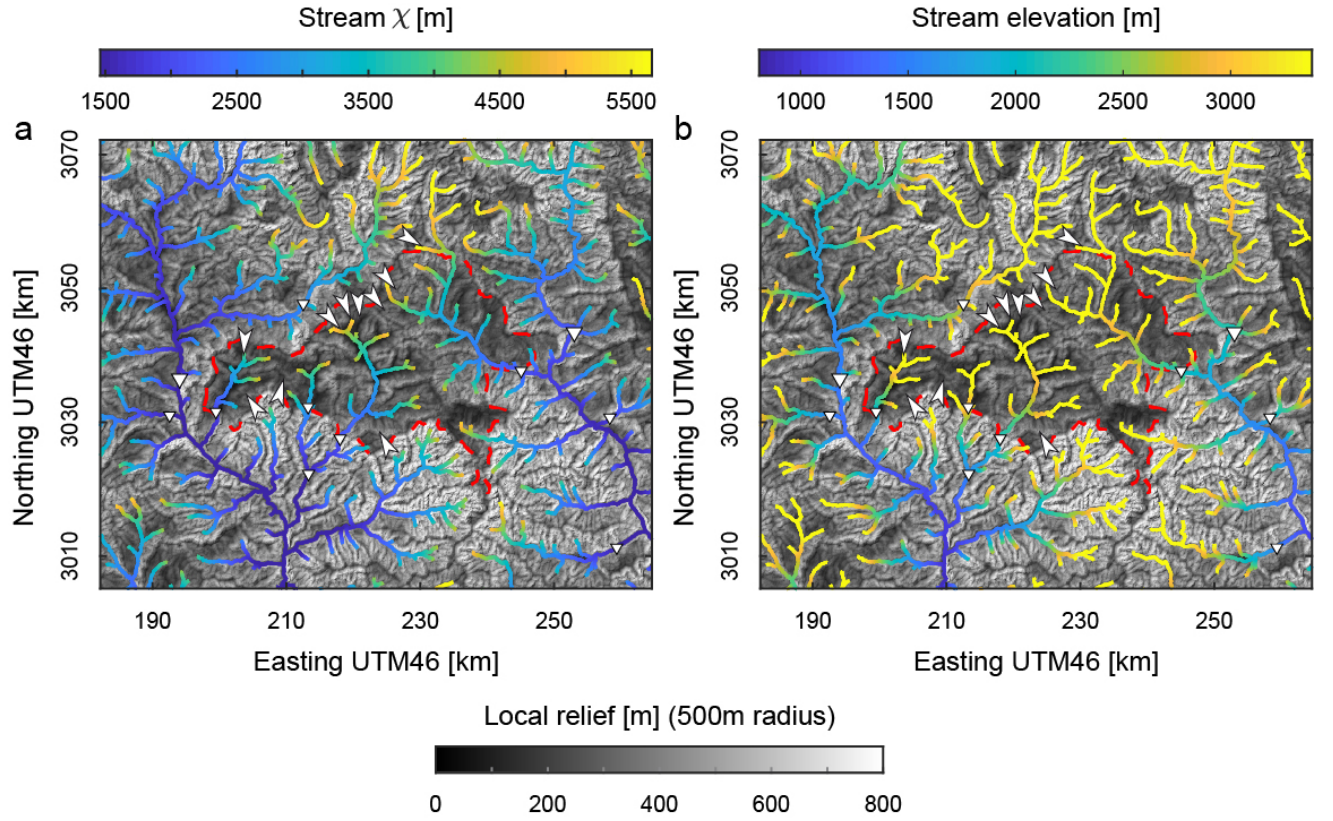


**Figure S6: Assessing divide mobility nearby the Phobijka high-altitude low-relief region** (see location on Figure 1c). Map represents local relief, with a moving window of 500 m, and the identified low-relief region is delimited by the red dashed line. Major knickpoints are reported with inversed triangles and arrows locate the existence of morphological observations of regressive erosion (wind gaps), together with the direction of the associated divide migration. Similar observations are reported for the Yarab region (Figure S7).

a)  $\chi$  along the river network as a criterium to assess divide mobility (following (Willett et al., 2014)). The values of  $\chi$  are determined for a concavity of 0.5. Same as map in Figure 9.

b) Stream elevation as a criterium to assess divide mobility (following (Forte and Whipple, 2018; Whipple et al., 2017b)).



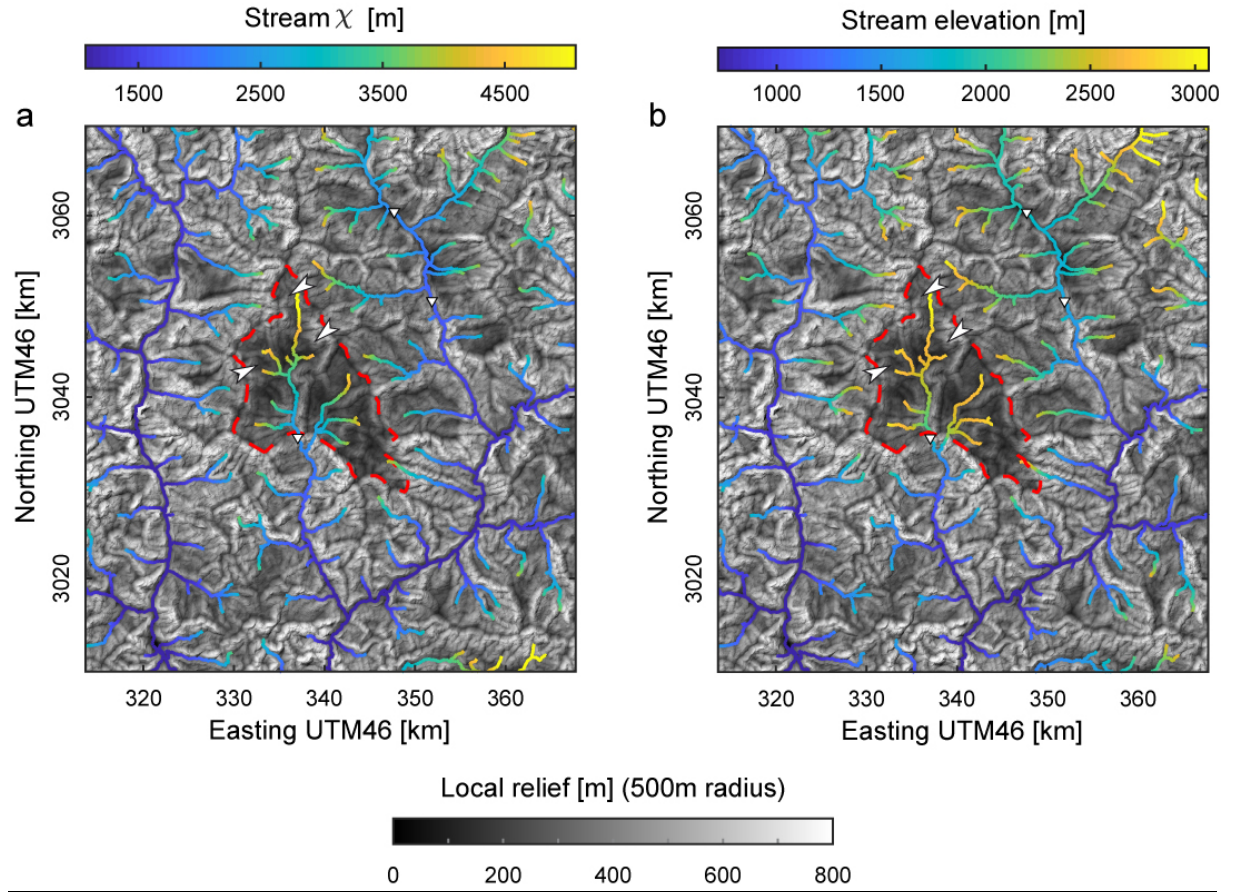


**Figure S7: Assessing divide mobility nearby the Yarab high-altitude low-relief region** (see location on Figure 1c), from Gilbert metrics. Map represents local relief, with a moving window of 500 m, and the identified low-relief region is delimited by the red dashed line. Major knickpoints are reported with inversed triangles and arrows locate the existence of morphological observations of regressive erosion (wind gaps), together with the direction of the associated divide migration. Similar observations are reported for the Phobijka region (Figure S6).

a)  $\chi$  along the river network as a criterium to assess divide mobility (following Willett et al. (2014)). The values of  $\chi$  are determined for a concavity of 0.5.

b) Stream elevation as a criterium to assess divide mobility (following Forte and Whipple (2018), and Whipple et al. (2017)).

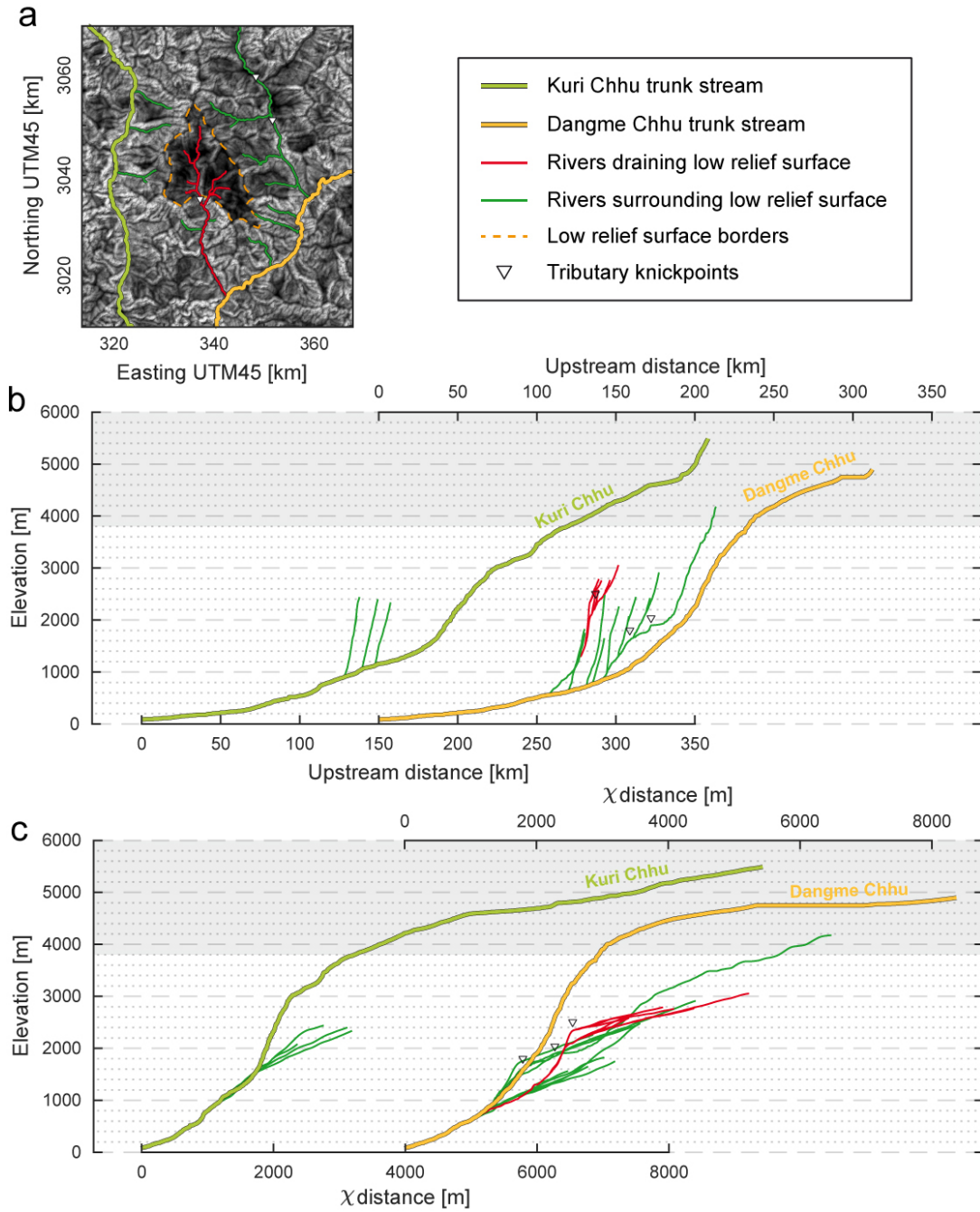


**Figure S8: Longitudinal and transformed river profiles around and within the Yarab high-altitude low-relief region**, following the approach of Yang et al. (2015). Comparable results are verified for the Phobjika region (Figure 8 in main text).

a) Map of topographic relief of the Yarab area (see Figure 1c for location), with a moving window of 500 m (scale bar as in Figure S7); the identified low-relief region is delimited by the orange dashed line. Major knickpoints are reported with inversed triangular symbols. Tributaries of the Kuri (west) and Dangme (east) Chhu trunk streams are color-coded, according to whether they drain the low-relief area (red) or are external to it (dark green).

b) Longitudinal river profiles of the Kuri and Dangme Chhu, with main tributaries draining (red) or external (dark green) to the low-relief Yarab area.

c) Transformed river profiles of the same rivers. Tributaries draining the low-relief area (red) plot above the main trunk streams as is observed in the case of area gain by river capture (Figure 4c). None of these profiles are concordant. Tributaries external to the low-relief area (dark green) are locally colinear with their main trunk stream, in particular in the case of the tributaries of the Kuri Chhu, even though they gain drainage area by progressive divide migration (Figure S7). The pattern is more complex for external streams that are tributaries of the Dangme Chhu, with some profiles above that of the local main trunk stream as in the case of river captures. This may be due to the existence of morphological relicts of former captures of low-relief areas, nearby the nowadays clearly identified Yarab surface. Indeed, some of these streams drain (relatively) lower relief regions external and east of the Yarab surface (Figure S8a).

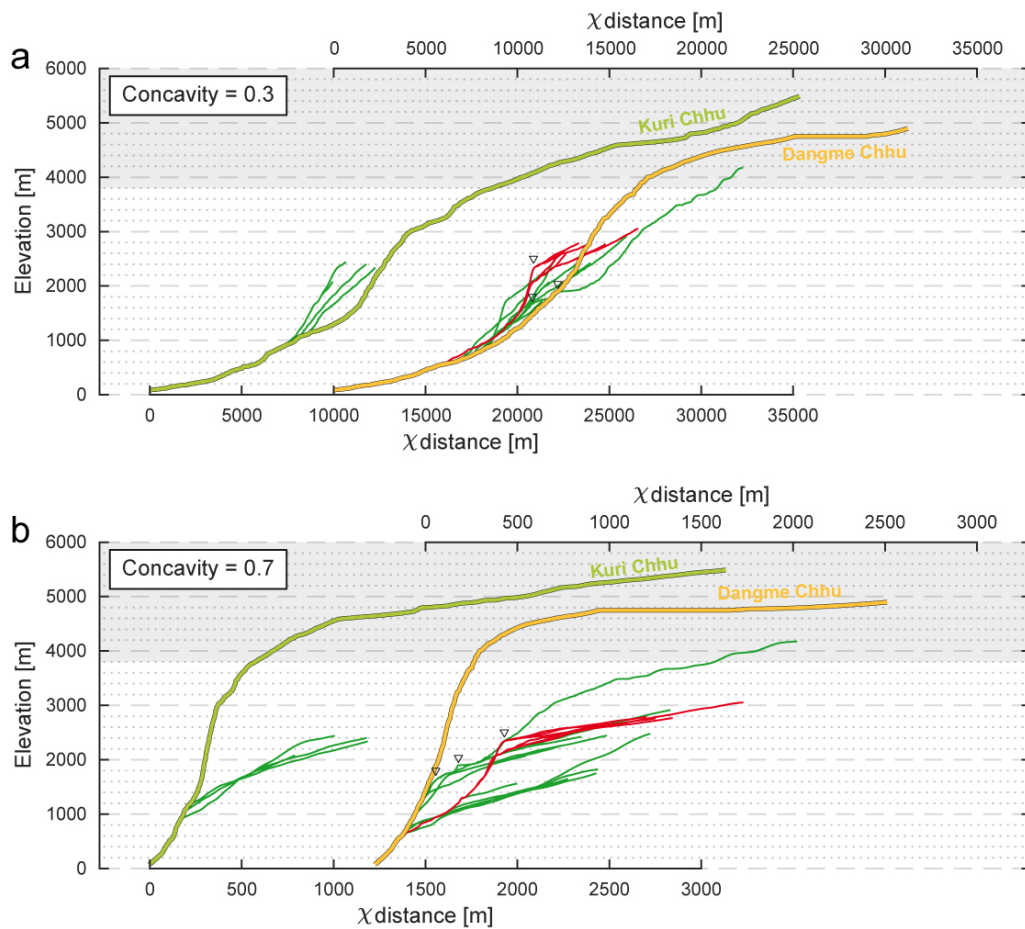


**Figure S9: Transformed river profiles around and within the Yarab high-altitude low-relief region,** following the approach of Yang et al. (2015) (see map of Figure S8). Concavity values of 0.3 (a- top) and 0.7 (b- bottom) are tested, complementing the transformed profiles of Figure S8c with a concavity of 0.5. Tributaries draining the low-relief area are represented in red. Tributaries external to the low-relief area are plotted in dark green. None of these profiles are concordant.

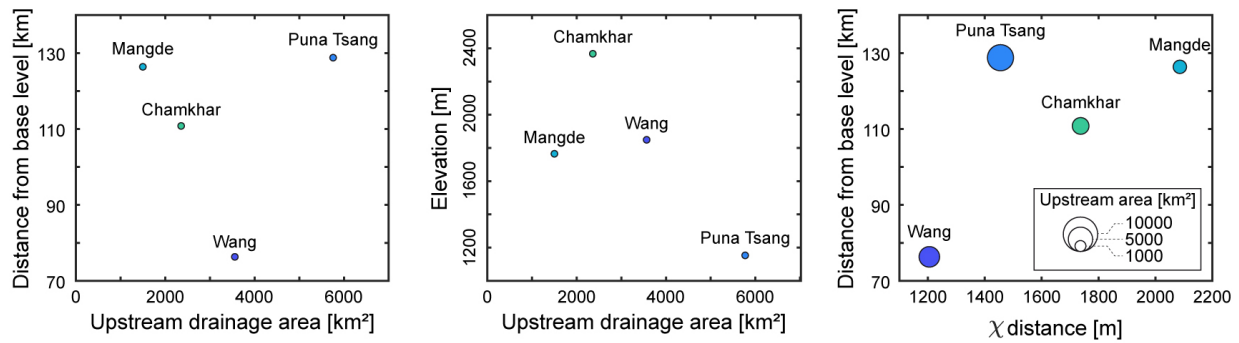


**Figure S10: Upstream distance (from base level) and elevation of major knickpoints in the case of major and large rivers, as a function of drainage area and transformed coordinates.** If the Wang Chhu is considered aside, the position of the knickpoints upstream the base level is independent of the drainage area (left). This is consistent with the fact that these knickpoints are all located along a consistent west-east band (Figures 1c and 5a in main text). In general, rivers with the smallest drainage basins have more elevated knickpoints (Chamkhar and Mangde Chhu) (center), most probably reflecting the fact that large rivers (Puna Tsang Chhu) tend to adjust better and/or faster to local forcing conditions. Finally, except for the Puna Tsang Chhu, upstream distance and  $\chi$  position of major knickpoints are positively correlated - but negatively correlated with drainage area - (right), an observation in contradiction with the idea that the discordance of transformed river profiles could reflect the impact of sediment flux in river incision (Giachetta and Willett, 2018).

## References

- Forte, A. M. and Whipple, K. X.: Criteria and Tools for Determining Drainage Divide Stability., *Earth and Planetary Science Letters*, 493, 102-117, <https://doi.org/10.1016/j.epsl.2018.04.026>, 2018.
- Giachetta, E. and Willett, S. D.: Effects of river capture and sediment flux on the evolution of plateaus: insights from numerical modeling and river profile analysis in the Upper Blue Nile catchment., *Journal of Geophysical Research*, 123, 1187-1217, <https://doi.org/10.1029/2017JF004252>, 2018.
- Perron, J. T. and Royden, L.: An integral approach to bedrock river profile analysis., *Earth Surface Processes and Landforms*, 38, 570-576, <https://doi.org/10.1002/esp.3302>, 2013.
- Whipple, K. X., Forte, A. M., DiBiase, R. A., Gasparini, N. M. and Ouimet, W. B.: Timescales of landscape response to divide migration and drainage capture: Implications for the role of divide mobility in landscape evolution, *Journal of Geophysical Research*, 122, 248-273, 2017.
- Willett, S. D., McCoy, S. W., Perron, J. T., Goren, L. and Chen, C. Y.: Dynamic reorganization of river basins, *Science*, 343, 1248765, <https://doi.org/10.1126/science.1248765>, 2014.
- Yang, R., Willett, S. D. and Goren, L.: In situ low-relief landscape formation as a result of river network disruption., *Nature*, 520, 526-529, <https://doi.org/10.1038/nature14354>, 2015.